Adsorption 11: 491–496, 2005

2D Automaton Simulation of Bubble Growth by Solute Diffusion in Correlated Porous Media

CARLOS FELIPE
Departamento de Química, Universidad Autónoma Metropolitana, Iztapalapa, P.O. Box 55-534, 09340 Mexico City, Mexico

RAÚL H. LÓPEZ AND ANA M. VIDALES
Departamento de Física, CONICET, Universidad Nacional de San Luis, 5700 San Luis, Argentina

ARMANDO DOMÍNGUEZ*
Departamento de Química, Universidad Autónoma Metropolitana, Iztapalapa, P.O. Box 55-534, 09340 Mexico City, Mexico
doar@xanum.uam.mx

Abstract. Simulations of bubble growth in porous media were carried out via a 2D numerical automaton built under a set of hypotheses derived from experimental observations at pore scale. Various types of 2D numerical networks (320×320 sites and corresponding bonds) were used as models of porous media to study the consequences of the spatial correlation length, ξ_{BB}, existing among the porous network void entities with respect to the growth of a gas cluster by solute diffusion occurring therein. The studied range was $\xi_{BB} \in [0.86 \pm 0.12,\ 10.63 \pm 0.12]$, in lattice units. The results obtained show that bubble development is truly affected by ξ_{BB}. The growth law exponent β changes as: $\beta = 4.95 - 0.53\,\xi_{BB} + 0.04\,\xi_{BB}^2$, while the fractal dimension of the gas cluster body, D_f, varies as: $D_f = 1.31 + 0.04\xi_{BB}$.

Keywords: automaton simulation, bubble growth, diffusion, porous media, spatial correlation

Introduction

Bubble growth by pressure drop of a gas-saturated liquid phase inside a porous medium plays a very important role in petroleum engineering for predicting the mass production during primary recovery (see e.g. Moulu, 1989). It has been established that the laws of bubble growth inside porous media are very different from those followed in bulk (see e.g. Li and Yortsos, 1995a); the differences arise from the fact that the evolution of the gas-liquid interfacial area is strongly influenced by the porous medium microstructure. In this scenario, the interaction between the different variables is complex (Domínguez et al., 2000), and the use of numerical tools is useful to discern the effects of the different variables, since this helps in the interpretation of experimental results and allows the virtual exploration of the system evolution. 2D simulations have been performed via a numerical automaton built under a set of hypotheses derived from experimental observations at pore scale on 2D micromodels. This automaton has been tested through comparison between experimental and numerical results; thereafter, the influence of liquid super-saturation, wettability and gravity has been investigated (Domínguez et al., 2000; Pérez-Aguilar et al., 2002). Now, the automaton is used in order to carry out a study on how the characteristics of the spatial void distribution existing within a porous

*To whom correspondence should be addressed.

network can influence the evolution of a gas cluster growing by solute diffusion inside it. Various types of 2D numerical networks have been used as models of porous media, these were built by using a variant of the dual site-bond model simulation framework (at this respect please c.f. Domínguez et al. (2001) and references therein). For the same pore-size distribution, this pore network simulation variant provides media endowed with different bond-to-bond size correlation lengths, ξ_{BB}. This manuscript reports the results of such study.

Method

The research method followed throughout this work can be divided in three parts: (i) construction of diverse types of numerical 2D square-lattice porous networks endowed with diverse degrees of spatial correlation among their void entities, (ii) characterization of their spatial size correlations through ξ_{BB}, and (iii) simulations of bubble growth in porous media by solute diffusion through a 2D numerical automaton.

Numerical Networks Construction

The porous medium is represented by a 2D square lattice of sites joined through bonds, as Fig. 1(a) illustrates. The geometrical characteristics of sites and bonds, in particular the sizes, R_b, and R_s of these void entities are illustrated in Fig. 1(b). While sites are conceived as cylindrical disks, bonds have rectangular prism geometry, since this shape allows the inclusion of solid wall roughness effects (liquid film) on bubble growth (see e.g. Perez-Aguilar et al., 2002). Also note that all network elements are assumed to possess the same channel depth h. A similar network construction procedure has been previously described in a detailed manner (Domínguez et al., 2001). This procedure is based on a Construction Principle (*CP*) that establishes that the size of any site should be larger or at least equal to the size of any of its connecting bonds, as well as on a parameter λ, which restricts the size differences existing among a pore and its neighbors. The building procedure allows the construction of assorted autoconsistent networks, i.e. both *CP* and λ restrictions are fulfilled. The simulated networks have void elements belonging to the same pore-size distribution but which are spatially distributed in different ways. A characteristic feature caused by the restrictions imposed on this model is the formation of "patches" of sites and bonds having the same sizes. The extent of these patches grows as correlations increase. The network is a 320×320 numerical matrix whose entries represent the sizes of the pore network constitutive elements (site, bond, and solid, where solid size $= 0$). The sizes of bonds and sites are chosen from prearranged log-normal population samples. The statistical parameters of the bond-size distribution include a mean size $\bar{R}_B = 10^{-4}$ m and a standard deviation $\alpha = 1.5 \times 10^{-5}$ m; these values were chosen from the experimental work of Wardlaw and Cassan, 1979, made on sandstone rock reservoirs. In turn, for sites the mean size $\bar{R}_S$ is chosen as 1.1×10^{-4} m and α is assumed to be the same as that of the bond population. The lattice spacing distance is imposed to be equal to 18.9×10^{-4} m with the purpose of simulating an experimental porosity value of 0.18 (Wardlaw and Cassan, 1979). Therefore, the average length of the bond population is $\bar{l}_B = 16.7 \times 10^{-4}$ m.

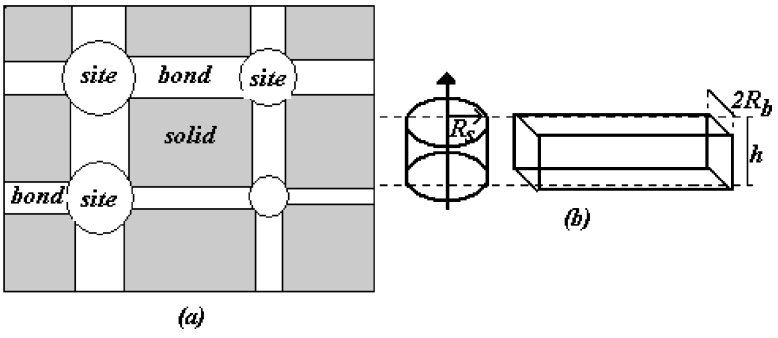

Figure 1. Structure of the numerical porous network. (a) Representation of a 2D square lattice of sites and bonds; (b) geometrical characteristics of constitutive elements: a site (left) and a bond (right).

Network Spatial Size Correlation

To investigate the way by which void elements are interconnected inside a simulated porous network, a correlation length is calculated (see e.g. Cordero et al., 2001). This quantity represents the mean extent (in lattice units) of patches where elements of similar sizes coexist. First, it is assumed that the size correlation coefficient, $C^{xy}(u)$, for two void elements x and y separated by a distance u (in lattice units) is defined through the following expression:

$$C^{xy}(u) = \frac{\langle (R_x - \bar{R}_x)(R_y - \bar{R}_y)\rangle}{[\langle (R_x - \bar{R}_x)^2\rangle \langle (R_y - \bar{R}_y)^2\rangle]^{1/2}} \qquad (1)$$

Where R represents the element size, and x, y being either S (a site) or B (a bond). This correlation function can be measured through Monte Carlo simulation by using a network of a finite size L. In this work, it is assumed that bonds control the capillary characteristics of the medium, that is why the spatial correlation of the void network is characterized via the bond-bond correlation length, ξ_{BB}, which is calculated by means of the expression proposed by Riccardo et al. (1993):

$$C^{BB}(u) = \exp\left(-\frac{u}{\xi_{BB}}\right) \qquad (2)$$

Where $C^{BB}(u)$ is the size correlation coefficient between two bonds separated by a distance u.

Gas Cluster Growth Simulation

The automaton employed in this work is based on a pore modeling technique and a set of hypotheses derived from experimental observations made on 2D transparent micromodels (Dominguez et al., 2000). A full description can be found in Pérez-Aguilar et al. (2002). The simulation assumes a porous network saturated with a liquid phase, under a uniformly distributed initial pressure P_0. Henry's law provides the initial uniform concentration of dissolved gas in the liquid phase as KP_0; K being Henry's constant. Next, an abrupt pressure drop ΔP is applied to the system and the generated gas super-saturation is enough to produce the nucleation of one bubble in a site which is then quickly and fully occupied by gas; this stage is considered instantaneous. Next, the gas phase grows under the combined effects of solute diffusion and porous medium capillarity, while the liquid phase pressure, $P = P_0 - \Delta P$, is kept constant. Gas cluster growth is idealized as a succession of slow pressurization steps at constant gas cluster volume, and instantaneous stages of gas volume expansion at constant gas mass. Thus, gas cluster growth rate can be conveniently computed through the duration of the pressurization periods, i.e., by knowing the time necessary for producing enough mass transfer into the bubble in order to create a critical pressure and to induce the movement of one or more menisci through neighbouring bond-site pairs. The thermodynamic conditions used for the simulation purposes of this work are $T = 293$ K, $P = 1$ bar, $\Delta P = 1.5$ bar, contact angle $\theta = 0^\circ$, in turn the thermodynamic values of the system CO_2-n-decane are surface tension $\sigma = 23.43 \times 10^{-3}$ N/m, $K = 4 \times 10^{-4}$ mole/Nm, and molecular diffusivity $D = 3.9 \times 10^{-9}$ m^2/s. The output results of the program are the gas cluster pattern, the time vector, the gas saturation vector, and the number of bonds vector of the gas cluster interface. In the next section, these results are presented showing the influence of porous network's topology on the phase distribution pattern and on the gas saturation temporal evolution, S_g.

Results and Discussion

Typical examples of results regarding the influence of ξ_{BB} on the pattern of a gas cluster are presented in Fig. 2, which shows the phase distribution of gas clusters occupying ~700 sites in three networks characterized by different ξ_{BB} values. According to Li and Yortsos (1995b) and Dominguez et al. (2000), such visualizations show the classic characteristics of clusters generated by an invasion percolation algorithm, i.e. irregular shapes together with some trapping of liquid phase. Note that the gas cluster shape goes from an irregular branched object to a dense disc, as ξ_{BB} increases. This is due to the gradual porous network structuralization as ξ_{BB} increases, i.e., a size-segregation effect progressively arises, this segregation effect means that regions of big entities linked together begin to appear and, in between them, there arise regions of smaller reunited pores (see e.g. Cordero et al., 2001). Thus, the characteristic extension of zones typified by a low capillary energy increases throughout the porous network as ξ_{BB} gets larger. This fact modifies the phase distribution because the gas phase grows seeking for the regions of the lowest capillary energy. The statistical ξ_{BB} error was estimated as 0.12. The gas cluster shape can be quantified via its fractal dimension, D_f (see e.g. Harrison, 1995). Its statistical variability was estimated

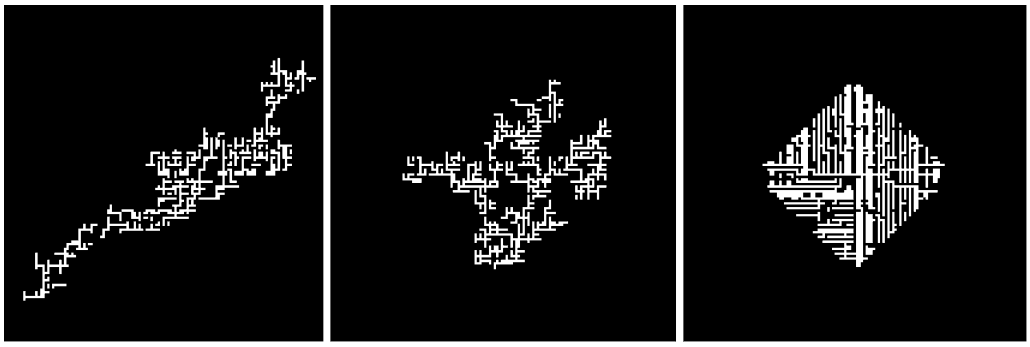

(a) (b) (c)

Figure 2. Phase distribution of a gas cluster (white) occupying ∼700 sites inside correlated porous networks. (a) $\xi_{BB} = 0.86 \pm 0.12$ and $D_f = 1.33 \pm 0.02$, (b) $\xi_{BB} = 4.53 \pm 0.12$ and $D_f = 1.55 \pm 0.02$ (c) $\xi_{BB} = 10.63 \pm 0.12$ and $D_f = 1.75 \pm 0.02$. These phase distributions correspond to the data presented in Fig. 3.

as 0.02. D_f goes from 1.33 ± 0.02 to 1.75 ± 0.02, while ξ_{BB} changes from 0.86 ± 0.12 to 10.63 ± 0.12, i.e. the gas phase fills the porous space more completely as ξ_{BB} gets bigger. This behavior is also observed in Fig. 3, where the dependence of β and D_f on ξ_{BB} is shown. Note the linear relationship arising between them. The best data fit is represented by: $D_f = 1.31 + 0.04\,\xi_{BB}$. β behavior will be explained below.

Concerning the S_g temporal evolution, it is pertinent to point out that the establishment of bubble growth laws in porous media is usually presupposed in the literature (see e.g. Moulu, 1989). For this reason, we analyze our results by means of the relationship $S_g \propto \tau^{\beta}$, where $\tau = Dt/\bar{l}_B^2$, t being the time of growth. This kind of analysis clearly shows the effects of different variables on bubble growth (see e.g. Perez-Aguilar et al., 2002). The volume (or S_g) of a single gas cluster tends to grow faster in porous media than in the bulk, i.e. a gas cluster grows via an exponent β greater than the values corresponding to the usual compact growth inside a homogeneous medium, $\beta = 1$ in 2D. The β values are obtained from simulated S_g versus time curves. In all cases, it has been clearly observed the establishment of a growth law after performing the gas invasion of the first 120 sites, this being the reason why the exponent β is calculated from a set of 150 to 1000 gas-invaded sites. The β statistical error is 0.09. It is pertinent to point out that the network size effect was not considered as a variable due to the following reasons: (i) the gas cluster size is always very small with respect to the network which can hold as many as 25,600 sites, and (ii) we have taken care that the gas phase is not interacting with the network boundary, i.e. if the gas cluster touches the network border then the corresponding virtual trial is discarded. The Fig. 3 shows significant differences concerning β values, when ξ_{BB} increases from 0.86 ± 0.12 to 10.63 ± 0.12. β values seem to be very sensitive to the evolution of the microstructure since first go down, from 4.63 ± 0.09 to 3.27 ± 0.09, as ξ_{BB} increases. But, the behavior changes when $\xi_{BB} = 7.98 \pm 0.12$, here β raises up to $\beta = 3.52 \pm 0.09$ as ξ_{BB} changes to $\xi_{BB} = 10.63 \pm 0.12$. To explain this behavior, it is necessary to consider that the time required for menisci progression is controlled by both gas mass transfer, and capillary constraint of the medium. If mass transfer is improved or capillary constraint is decreased, then bubble growth is enhanced. Mass transfer depends on the solute concentration field around the gas cluster. Meniscus progression represents a partial renovation of

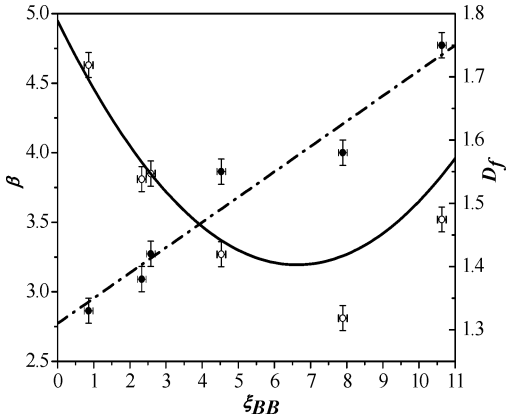

Figure 3. Pore network simulation on correlated networks: (a) The influence of ξ_{BB} on β, best fit (continuous line) $\beta = 4.95 - 0.53\,\xi_{BB} + 0.04\,\xi_{BB}^2$, and (b) the influence of ξ_{BB} on D_f, best fit (dash dot line) $D_f = 1.31 + 0.04\xi_{BB}$.

the concentration gradient around gas cluster, if a bond at the gas cluster boundary is drained of liquid then three or two additional super-saturated bonds are incorporated to the cluster boundary. From this perspective, ξ_{BB} hinders mass transfer since the area of influence of the gas cluster is reduced as ξ_{BB} grows, i.e. in lowly correlated networks the liquid-gas menisci progress towards gas super-saturated areas, while in highly correlated networks the liquid-gas interface evolves inside a relatively small area then producing the local annihilation of the gas super-saturation. On the other hand, with respect to capillary restrictions, in lowly correlated networks gas cluster borders are characterized by a more heterogeneous population of capillary thresholds due to a random repartition of network entities; in contrast to this behavior, pore-size structuralization in correlated networks overcomes the above random size repartition and the size-segregation effect allows a quicker cluster growth (i.e. a larger β value), because the mean capillary threshold in a higher correlated network is smaller than in a non-correlated one, thus improving bubble growth. As it can be seen in Fig. 3, the combination of these two effects produces a non-linear variation of β as function of ξ_{BB}. Data fit renders the following relationship: $\beta = 4.95 - 0.53\,\xi_{BB} + 0.04\,\xi_{BB}^2$.

Conclusion

2D numerical simulation was used in order to analyze the effects of porous network spatial correlations on bubble growth in porous media; this variable being difficult to study experimentally. The numerical analysis developed here about the growing rate of an isolated single gas cluster by solute diffusion in correlated porous networks indicates that network topology exerts a significant influence on both gas cluster growth, $\beta = 4.95 - 0.53\,\xi_{BB} + 0.04\,\xi_{BB}^2$, and gas cluster morphology, $D_f = 1.31 + 0.04\xi_{BB}$.

Some refinement of the automaton should be made in order to arrive to a model of practical use. Future work includes:

1. The study of connectivity effects (not considered here). It is known that a capillary process occurring inside a porous medium is strongly affected by the connectivity of the medium (Cordero et al., 2001; Rojas et al., 2002). Connectivity promotes spatial size-segregation of pore elements, the bigger the connectivity is the more compact the gas cluster shape is. With respect to cluster growth kinetics, the balance of inhibitory (a limited zone of influence) and promotive (low or medium capillary constriction) should result in a non-linear relationship between connectivity and β. Quantitative verification of these likely trends is the goal of future work.
2. In general, the study of the dimensionality effects (restricted here to 2D) is integrated in the study of the connectivity effects when gravity is neglected. Thus, it would be interesting to develop a 3D version of the simulator, especially for situations where gravity effects are important.
3. The implementation, in the simulator, of simultaneous nucleation and growing of various gas clusters.

Finally, in spite of its limitations, the numerical tool here developed has been very useful to study the influence of diverse parameters about gas cluster behavior.

Acknowledgment

Thanks are given to CONACyT (México)-CONICET (Argentina) for financing the joint Project "Catalysis, Fisicoquímica de Superficies e Interfases Gas-Sólido".

References

Cordero, S., F. Rojas, and J.L. Riccardo, "Simulation of Three-Dimensional Porous Networks," *Coll. and Surf. A*, **187/188**, 425–438 (2001).

Domínguez, A., S. Bories, and M. Prat, "Gas Cluster Growth by Solute Diffusion in Porous Media. Experiments and Automaton Simulation on Pore Network," *IJMF*, **26**, 1951–1979 (2000).

Domínguez, A., H. Pérez-Aguilar, F. Rojas, and I. Kornhauser, "Mixed Wettability: A Numerical Study of the Consequences of Porous Media Morphology," *Coll. and Surf. A*, **187/188**, 415–424 (2001).

Harrison, A., *Fractals in Chemistry*, Oxford University Press, New York, pp. 16–17, 1995.

Li, X. and Y.C. Yortsos, "Theory of Multiple Bubble Growth in Porous Media by Solute Diffusion," *Chem. Eng. Sci.*, **50**, 1247–1254 (1995a).

Li, X. and Y.C. Yortsos, "Visualization and Simulation of Bubble Growth in Pore Networks," *AIChE J.*, **41**, 214–222 (1995b).

Moulu, J.C., "Solution-Gas Drive: Experiments and Simulation," *J. Pet. Sci. Eng.*, **2**, 379–386 (1989).

Pérez-Aguilar, H., A. Domínguez, C. Rodríguez, F. Rojas, and I. Kornhauser, "Virtual Study of Wettability Effects on Bubble Growth by Solute Diffusion in Correlated Porous Networks," *Coll. and Surf. A*, **206**, 179–192 (2002).

Riccardo, J.L., V. Pereyra, G. Zgrablich, F. Rojas, V. Mayagoitia, and I. Kornhauser, "Characterization of Energetic Surface

Heterogeneity by a Dual Site-Bond Model," *Langmuir*, **9**, 2730–2736 (1993).

Rojas, F., I. Kornhauser, C. Felipe, J.M. Esparza, S. Cordero, A. Domínguez, and J.L. Ricardo, "Capillary Condensation in Heterogeneous Mesoporous Networks Consisting of Variable Connectivity and Pore-Size Correlation," *PCCP*, **4**, 2346–2355 (2002).

Wardlaw, N.C. and J.P. Cassan, "Oil Recovery and the Rock-Pore Properties of Some Sandstone Reservoirs," *Bul. Can. Petroleum Geol.*, **27**, 117–138 (1979).